JOURNAL OF GEOPHYSICAL RESEARCH, VOL. 99, NO. A11, PAGES 21,419–21,427, NOVEMBER 1, 1994

Interplanetary magnetic field collimated cosmic ray flow across magnetic shock from inside of Forbush decrease, observed as local-time-dependent precursory decrease on the ground

K. Nagashima and K. Fujimoto

Cosmic-Ray Section, Solar-Terrestrial Environment Laboratory, Nagoya University, Nagoya, Japan

I. Morishita

Department of Information Management, Asahi University, Hozumi-cho, Motosu-gun, Gifu, Japan

Abstract. In the previous papers (Nagashima et al., 1992, 1993) the authors pointed out the existence of the local-time-dependent precursory decrease of cosmic rays in front of the shock wave of the interplanetary magnetic field (IMF) and interpreted it as being due to the IMF-collimated outward flow of the low-density cosmic rays across the shock from the inside of the Forbush decrease. In those papers, however, the physical properties of the collimated flow such as the direction, the collimation angle, and the rigidity spectrum of the constituent cosmic rays were only estimated qualitatively owing to the lack of the simulation of the precursory decrease produced by the flow. In the present paper these properties are quantitatively obtained by analyzing the hourly data of the precursory decreases observed on January 25 and 26, 1968, at the worldwide neutron monitor stations. The obtained direction and collimation angle of the flow approximately coincide respectively with those expected from the IMF. This fact gives evidence for the reconfirmation of the existence of the IMF-guided collimated flow, responsible for the precursory decrease.

1. Introduction

The local-time-dependent precursory decrease of cosmic rays, observed in front of the magnetic shock wave, is produced by the interplanetary magnetic field (IMF)-collimated outward flow of the low-density cosmic rays across the shock from the inside of the Forbush decrease (FD) [*Nagashima et al.*, 1992, 1993]. The collimation of the flow is due to the bottle-neck structure of the magnetic field at the shock front, and the constituent cosmic rays of the flow have the pitch angle with the magnetic field less than or equal to χ_O, defined by the following equation:

$$\sin^2 \chi_O = B_O/B_S, \tag{1}$$

where B_S and B_O are the magnetic field strengths at the shock front and the observation point, respectively. In the present paper we obtain the physical properties of the flow, such as the geographic direction (λ_F, ϕ_F), the collimation index (χ_O), and the rigidity spectrum $\{S(p)dp\}$ of the constituent cosmic rays by analyzing the hourly data of the precursory decrease from the worldwide neutron monitor stations.

2. Precursory Decrease

The data used for the present analysis of the precursory decrease (PD) are those from 51 stations as listed in Table 1 on January 25 and 26, 1968, before the appearance of the moderate FD caused by the magnetic shock wave. Some of the PDs observed at several stations are shown in Figure 1, together with the IMF and the solar wind velocity [*Couzens and King*, 1986]. The commencement time of the magnetic shock was about 1400 UT on January 26. Lagging behind the shock, the FD started at 2100 UT at the Arctic station Thule (geographic latitude $\lambda = 76.6°$N, longitude $\phi = 291.1°$E) and 1800 UT at the Antarctic station Wilkes ($\lambda = 66.4°$S, $\phi = 110.5°$E), as shown on the lower part in Figure 1. As the intensity at these stations is not much disturbed by the usual daily variation owing to their high-latitude location, it can be used for the accurate determination of the commencement of FD. In the present case, however, the commencements at these stations were not at the same time. This is due to the superposition of the additional flux on the FD at the Arctic station, which is produced by the cosmic ray southward anisotropy along the IMF nearly perpendicular to the ecliptic plane during the period 1700–2200 UT on January 26 [cf. *Couzens and King*, 1986]. The existence of such a north-south anisotropy along IMF nearly perpendicular to the ecliptic plane has been recently found out during the Forbush decrease by two of the present authors (K.N. and K.F.). The detailed description of the anisotropy will be reported elsewhere. At present, we regard 1800 UT as the commencement time of the FD. Such a consideration on the commencement of the FD has been made in order to show that the PDs are observed earlier than the FD and not a part of it. Almost all the observed PDs satisfy this condition, except for some special cases as will be mentioned later. The PDs in Figure 1 are plotted from top to bottom in the west-longitudinal order of the stations so that one can easily recognize their local time dependence. It is noted that some of them still keep decreasing even after the occurrence of the

Paper number 94JA01224.
0148-0227/94/94JA-01224$05.00

Table 1. The Minimum (ΔI_m) of the Precursory Decreases and Its Occurrence Time (t_m) Listed From Top to Bottom in the West-Longitudinal Order of the Station on January 25 and 26, 1968

	Station	ϕ, deg	λ, deg	p_c, GV	σ_h, %	$\lvert\Delta I_m\rvert$, %		t_m (UT)	
						Jan. 25	Jan. 26	Jan. 25	Jan. 26
1	South Pole	0.0	−90.0	0.09	0.35		0.51		11.5
2	Leeds	358.4	53.8	2.17	0.20		1.14		6.5
3	Sanae	357.6	−70.3	0.91	0.44		2.08		8.5
4	Goose Bay	299.6	53.3	0.60	0.22		1.56		12.0
5	Cordoba	295.8	−31.4	10.73	1.19		2.75		11.5
6	Mina Aguilar	294.3	−23.1	12.51	0.35		2.14		9.5
7	Chacaltaya	291.8	−16.3	12.62	0.13	...	2.11	...	8.5
8	Ushuaia	291.7	−54.8	5.27	0.75		1.95		9.0
9	Thule	291.1	76.6	0.00	0.26				
10	Durham	289.2	43.1	1.57	0.21		3.03		12.0
11	Mount Washington	288.7	44.3	1.38	0.43		2.77		12.0
12	Huancayo	284.7	−12.0	13.01	0.38		2.22		8.5
13	Swathmore	284.6	39.9	1.95	0.28		2.84		12.5
14	Ottawa	284.4	45.4	1.08	1.08		3.07		13.0
15	Deep River	282.5	46.1	1.07	0.13		3.32		12.5
16	Chicago	272.3	41.8	1.75	0.87		3.32		11.5
17	Churchill	265.9	58.8	0.20	0.19		0.96		12.5
18	Resolute Bay	265.1	74.7	0.00	0.34				
19	Dallas	263.3	33.0	4.11	0.21		3.16		11.0
20	Climax	253.8	39.4	2.97	0.26		3.27		12.5
21	Calgary	245.9	51.1	1.07	0.24		2.56		13.5
22	Sulpher Mount	244.4	51.2	1.09	0.46		2.68		13.5
23	Victoria	236.7	48.4	1.75	0.27	...	2.59	...	13.5
24	Inuvik	226.3	68.4	0.16	0.19		0.96		16.5
25	Kula	204.7	20.7	12.97	0.47	1.42	2.09	18.0	10.5
26	McMurd Sound	166.6	−77.9	0.00	0.19				
27	Brisbane	153.1	−27.4	7.00	1.20	1.35	2.01	21.5	16.5
28	Hobart	147.3	−42.9	1.80	0.81	1.62*	2.59†	20.5*	16.5†
29	Terre Adelie	140.0	−66.7	0.01	0.75				
30	Mount Norikura	137.6	36.1	11.36	0.42	1.27	1.09†	17.5	16.5†
31	Yakutsk	129.7	62.0	1.63	1.57	3.07	0.00†	22.5	16.5†
32	Tixie Bay	128.9	71.6	0.45	0.27	0.70*	0.74†	21.5*	16.5†
33	Wilkes	110.5	−66.4	0.01	0.70				
34	Irukutsk	104.0	52.5	3.56	0.23	1.08	0.54†	21.5	16.5†
35	Alma Ata	76.9	43.3	6.61	0.72		1.35		0.0
36	Kerguelen Island	70.3	−49.4	1.10	0.37		1.92		1.5
37	Mawson	62.9	−67.6	0.19	0.74		1.90		2.5
38	Heiss Island	58.1	80.6	0.08	0.67				
39	Tbilisi	44.8	41.7	6.66	0.68		1.97		0.5
40	Kampala	32.6	0.3	14.98	0.70		2.02		3.5
41	Oulu	25.5	65.1	0.77	0.29		0.85		2.5
42	Hermanus	19.2	−34.4	4.56	0.50		2.09		4.5
43	Uppsala	17.6	60.0	1.34	0.64		1.50		3.5
44	Rome	12.5	41.9	6.24	0.27		0.50		3.0
45	Halle	12.0	51.5	3.10	1.27		1.54		4.5
46	Munich	11.6	48.2	4.14	0.46		0.96		3.5
47	Zugspitze	11.0	47.4	4.31	0.33		1.40		4.5
48	Lindau	10.1	51.7	2.99	0.57		0.82		3.5
49	Kiel	10.1	54.3	2.32	0.22		0.94		4.0
50	Jungfraujoch	8.0	46.6	4.53	0.27		0.73		4.0
51	Pic Du Midi	0.2	42.9	5.48	0.16		0.93		4.5

*Not certain.

†The value at 1630 UT as no minimum peak is found owing to the merging of the precursory decreases into the Forbush decrease (cf. text).

Here ϕ, east longitude; λ, latitude; p_c, cosmic ray geomagnetic cutoff rigidity; σ_h, dispersion derived from the hourly fluctuation of the cosmic ray flux. Three center dots indicate no data.

magnetic shock at 1400 UT. This indicates that the collimation of the cosmic rays is already produced inside the magnetic shock, as has been pointed out previously [*Nagashima et al.*, 1992]. It is also noted that two concavities observed at Kula (λ = 20.7°N, ϕ = 204.7°E) for 2 days running could be regarded as the successive PDs (cf. Figure 1). Such a phenomenon was also observed at several stations as will be shown later in Table 1. The successive PDs have been observed recently also with the 17 directional muon telescopes at Nagoya (λ = 35°N, ϕ = 137°E) on September 7 and 8, 1992 [*Nagashima et al.*, 1993].

The observed PDs are different from each other in their time profile. Generally, the profile depends chiefly upon the latitude of the station; in the high latitudes it shows a sudden decrease and recovery within a short duration period, while in the low latitudes, it shows a gradual decrease and recovery over a long duration period. As an example, we show in Figure 2 the PDs observed at Chacaltaya (λ = 16.3°S, ϕ =

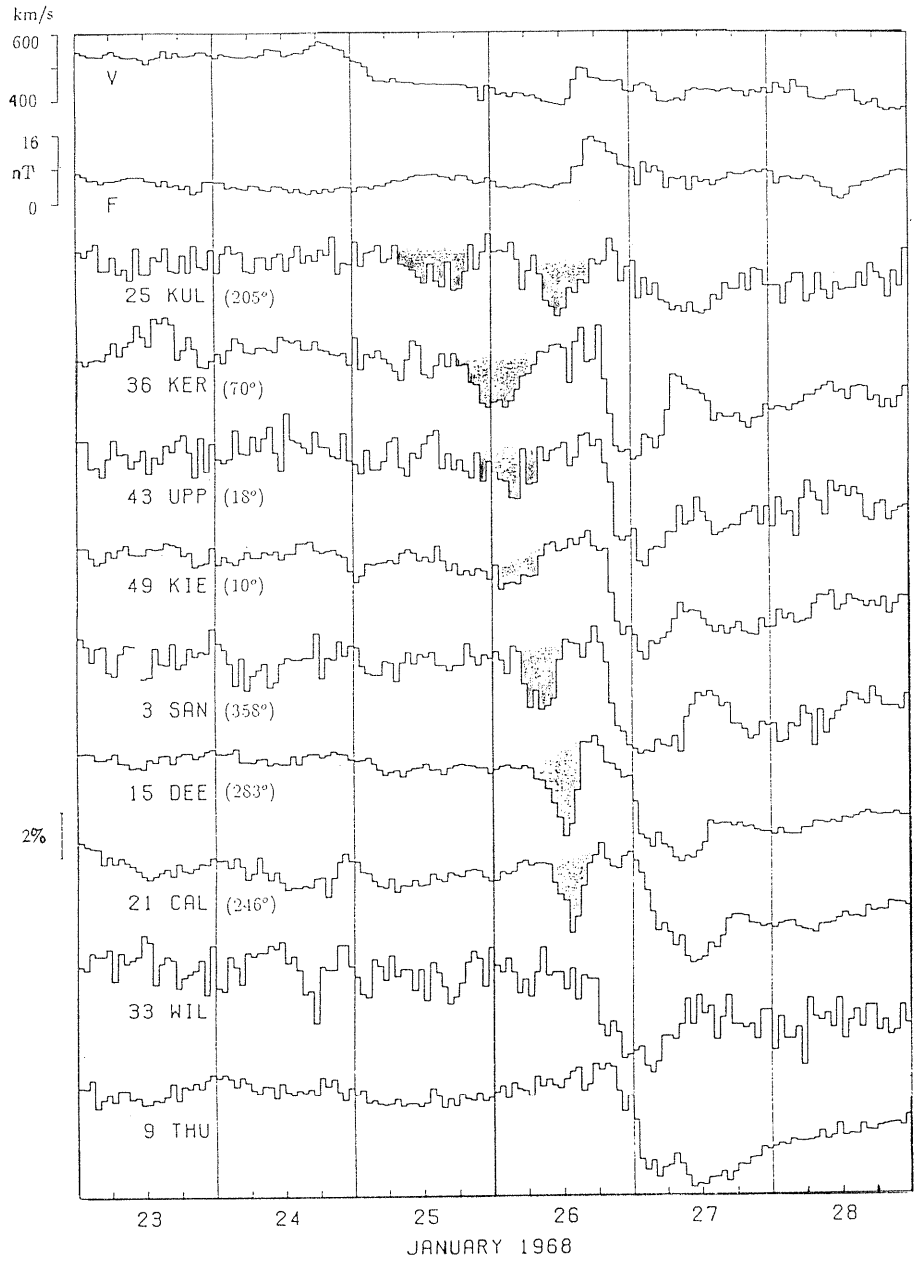

Figure 1. Local-time-dependent precursory decrease (PD) of cosmic ray neutron intensity in front of the magnetic shock wave responsible for the Forbush decrease. The shaded region indicates the decrease. The figures and letters attached to the intensities express the observation station and its east longitude listed in Table 1. The intensities at Thule and Wilkes in the lower part do not show any precursory decrease but are presented here in order to show the commencement time of the Forbush decrease. F, the interplanetary magnetic field; V, the solar wind velocity [*Couzens and King*, 1986].

291.8°E; geomagnetic cutoff rigidity p_c = 12.62 GV) and Sanae (λ = 70.3°S, ϕ = 357.6°E; p_c = 0.91 GV), together with the trajectory of the geomagnetic asymptotic orbital directions of the cosmic rays for various rigidities (p values) at these stations, which will be called hereafter the trajectory at the station, for simplicity. The duration period at Chacaltaya is almost twice as long as that at Sanae. Because of its long-duration period, the time profile at Chacaltaya is very similar to the daily variation usually observed and can hardly be recognized as the PD without the aid of the information from other stations. Such a difference in the duration period is caused by the difference in the modulus ($d\phi/dp$) of the longitudinal spread of the trajectory shown in Figure 2. Owing to the large modulus, the neutron telescope at Chacaltaya has a wide longitudinal field of vision and therefore, even if the flow has a very small collimation index (χ_O), the telescope can successively observe, for many hours, the constituent cosmic rays of the flow in a limited rigidity range shifted from low to high rigidity with the rotation of the Earth. As a result, the PD shows a shallow and wide concavity with a gradual decrease and recovery, as observed. The PD at Kula in Figure 1 also belongs to this

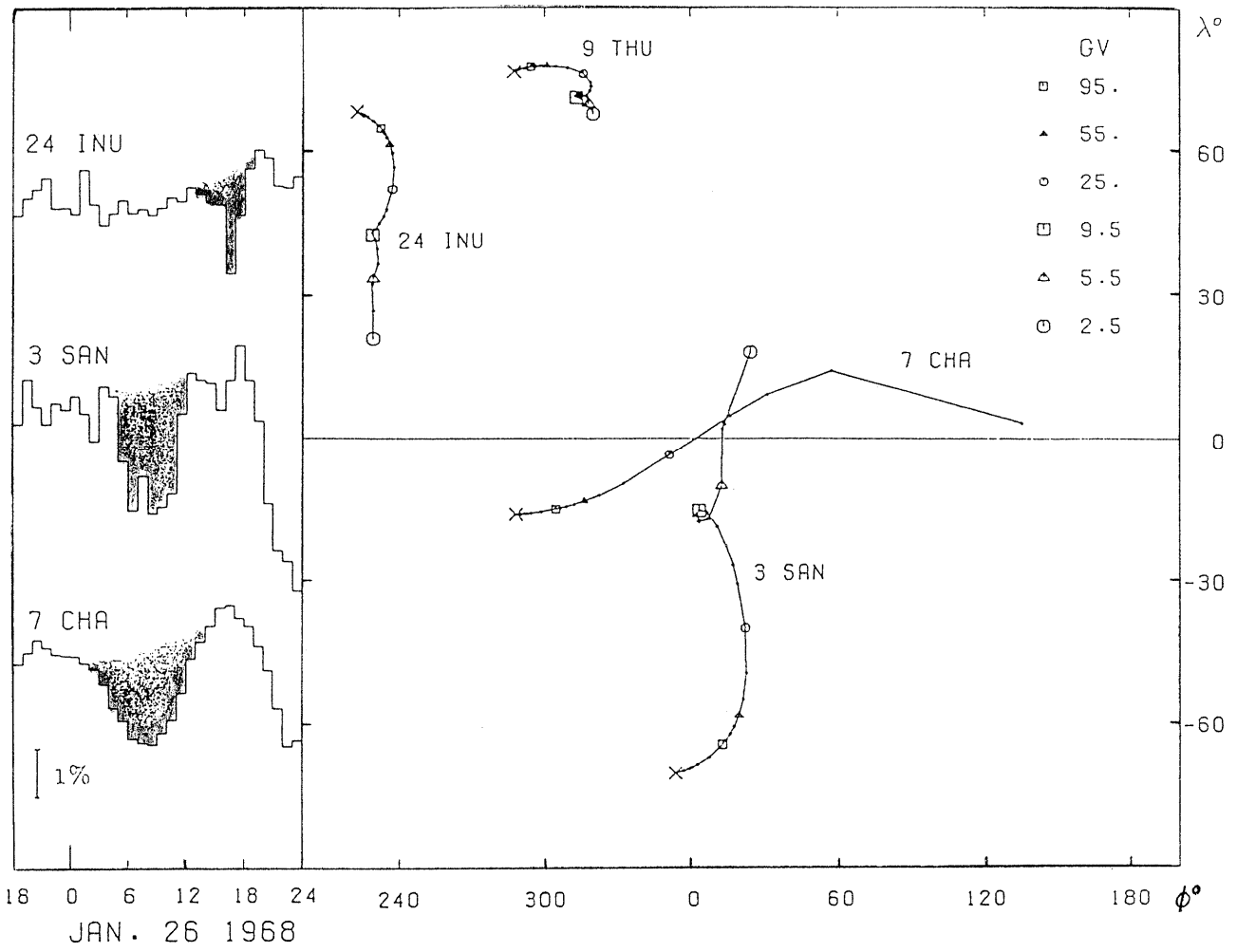

Figure 2. PD at Chacaltaya, Sanae, and Inuvik (on the left), and the trajectories of the asymptotic orbital directions of the cosmic rays with rigidity (p) in the geomagnetic field at these stations (on the right), quoted from *Inoue et al.* [1983]. The shaded region indicates the decrease. The figures and letters attached to the intensities express the station listed in Table 1. The station on the map is expressed by the cross point and the asymptotic direction for the rigidity (p) is shown by the character figure designated on the right.

category. On the other hand, the telescope at Sanae has a narrow field of vision ($\Delta\phi_T$) less than about 30° and can observe the cosmic rays of the flow in a wide rigidity range almost at the same time. As a result, the PD shows a deep and narrow concavity with a sudden decrease and recovery, as shown in the figure. In such a case we can approximately determine the collimation index (χ_O) by subtracting $\Delta\phi_T$ from the duration period ($\Delta\phi_P$) of the PD, as

$$\chi_O = (\Delta\phi_P - \Delta\phi_T)/2. \quad (2)$$

As $\Delta\phi_P = 105°(=7\ h)$ and $\Delta\phi_T \leq 30°$, we get $\chi_O \geq 37.5°$. On the same figure, we show also the intensities and the trajectory at Inuvik ($\lambda = 68°$N, $\phi = 226.3°$E; $p_c = 0.16$ GV), for reference. The trajectory at this station is very similar in shape to that at Sanae, but it is confined in the region narrower in longitude and higher in latitude than the latter. Because of this difference, the Inuvik station can observe only a small and narrow PD due to the low-rigidity cosmic rays from the collimated flow in the low latitudes. The large magnitude differences among the PDs in Figure 1 also are mainly due to the latitudinal difference of the trajectories for the cosmic rays, which effectively contribute to the neutron intensity. As one of the most extreme trajectories, we show the one at Thule in Figure 2. Owing to the concentration of the trajectory in the polar regions, the intensity at the station does not show any definite response to the collimated flow except for a very tiny and doubtful dip at 1500–1700 UT on January 26, as shown in Figure 1. On the basis of this fact we have used the neutron intensity at this station for the determination of the commencement of FD. In the middle latitudes, on the other hand, the trajectory is composed of two parts, one is of the Sanae type in the high-rigidity region and the other is of the Chacaltaya type in the low-rigidity region. The time profile of the PD is determined by the type of the partial trajectory for the rigidities of the cosmic rays, which most effectively contribute to the decrease. Therefore, in the middle latitudes we could observe the PD of three types, that is, the Sanae type, the Chacaltaya type, and the intermediate type. In case of the last type the time profile shows a gradual decrease and a rapid recovery as the

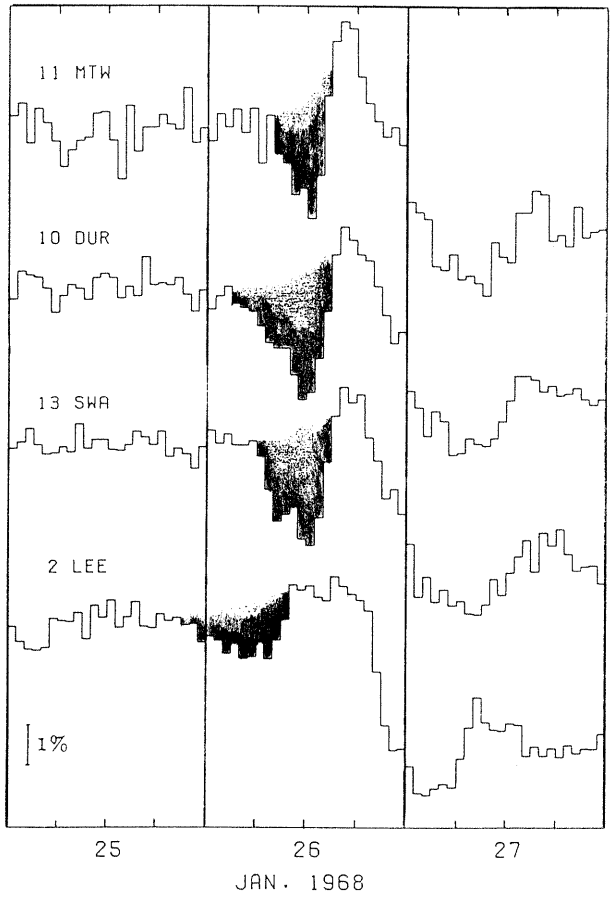

Figure 3. Precursory decrease at the middle-latitude stations, characterized with a gradual decrease and a rapid recovery. The figures and letters attached to the intensities express the observation station listed in Table 1. The shaded region indicates the decrease.

telescope first observes the low-rigidity cosmic rays with the trajectory of the Chacaltaya-type. Such a tendency can be recognized in the observation at Deep River (λ = 46.1°N, ϕ = 282.5°E) in Figure 1 and also at those stations in Figure 3. In the following we obtain the cosmic ray flow in space responsible for these PDs.

3. Analysis

The hourly value $\Delta I(t)$ of the PD for the present analysis is obtained as follows: we first calculate the 3-hour running averages of the neutron intensities in order to reduce hourly fluctuations due to the statistical errors and then take the deviation $\{\Delta I(t)\}$ from the level line through the start and end points of the duration period of the PD determined at each station at our own discretion. All the $\Delta I(t)$s outside the period are set zero in order to avoid the disturbance due to other causes. The minimum (ΔI_m) among $\Delta I(t)$s and its occurrence time (t_m) thus obtained are shown in Table 1, for reference. At some stations in the table, ΔI_m and t_m are substituted by the respective values at the center of the duration period, as t_m is extremely near the end of the period owing to the large statistical fluctuation of $\Delta I(t)$s. The stations are listed from top to bottom in west-longitudinal order of their location, so that the longitudinal dependence of t_m can be easily seen. Some disorderliness in the sequence of t_m in the table is mainly due to the difference of the latitudes or the heights of the stations, in other words, the difference of the longitudinal deflections of the effective cosmic rays in the geomagnetic field. The affix (†) to ΔI_m and Δt_m indicates that the PD does not show the minimum peak owing to its merging into the FD in spite of its earlier appearance than the FD [cf. *Nagashima et al.*, 1992]. In this case, ΔI_m expresses the deviation at 1630 UT from the horizontal level line through the start point of the period of the PD. It is emphasized here that, owing to the merging, the PD is apt to be mistaken for the earlier occurrence of the FD than other station's or to be regarded as a result of the malfunction of the cosmic ray telescope.

As the PD is observed at many stations at the same time, we can infer, without any precise analysis, the direction of the flow and its collimation index (χ_O) from the geographic distribution of the cosmic ray trajectories classified by the presence or absence of $\Delta I(t)$ at the stations at a time t. An example of the distribution at 0830 UT January 26 is shown in Figure 4, in which the thick or thin trajectory indicates the presence or absence of $\Delta I(t)$ at the station expressed by the numbered cross. The dashed circle in Figure 4 expresses a tentative boundary of the collimated flow, its center (λ_F = 0°, ϕ_F = 20°E) and radius (37.5°) being inferred from the time variation of $\Delta I(t)$ at the number 3 station Sanae, as follow. The radius is equated to the lower limit of χ_O previously estimated from the period of $\Delta I(t)$ at Sanae. The direction of the center must be in the meridian plane specified by average longitude of the trajectory at Sanae, as the selected epoch (0830 UT) is the midperiod of $\Delta I(t)$ at the station (cf. Figures 2 and 4). Its latitude (λ_F), on the other hand, cannot be determined in such a way and is tentatively assumed to be at the equator, as IMF is usually not far from this direction. As can be seen in Figure 4, almost all the thick lines focus into or pass across the circular region, while almost all the thin lines detour around the region, indicating that the above estimate of the region of the collimated flow seems reasonable. Strictly speaking, it is more reasonable to assume a little larger circular region with its center a little southwestward from the present point, so that it can include a part of the trajectories at South Pole, Mawson, and Leeds (numbers 1, 37, and 2), but not include those at the European stations (numbers 39, 41, and 43–51). It is emphasized that the difference between the presence of the PD at the number 2 station Leeds and its absence at other European stations is caused by a very small longitudinal difference in their trajectories. This indicates the existence of a very sharp boundary of the collimated flow.

In the above inference we have used only those trajectories for somewhat high rigidities, in order to prevent complexity of their geographic distribution. The eliminated trajectories are those for the rigidities less than 2.5 GV at the stations with the geomagnetic cutoff rigidity (p_c) less than 2.5 GV and also for the rigidities near p_c at low-latitude stations with $p_c \geq 2.5$ GV; some of them pass across the circular region in spite of the absence of $\Delta I(t)$, for example, at the stations Brisbane, Mount Norikura, and Victoria (numbers 27, 30, and 23 in Figure 4 and Table 1). Such an elimination of the included trajectories in the region, however, does not affect materially the above mentioned inference, because the contribution of the cosmic ray flux from the circular region to $\Delta I(t)$ is very small owing to the small

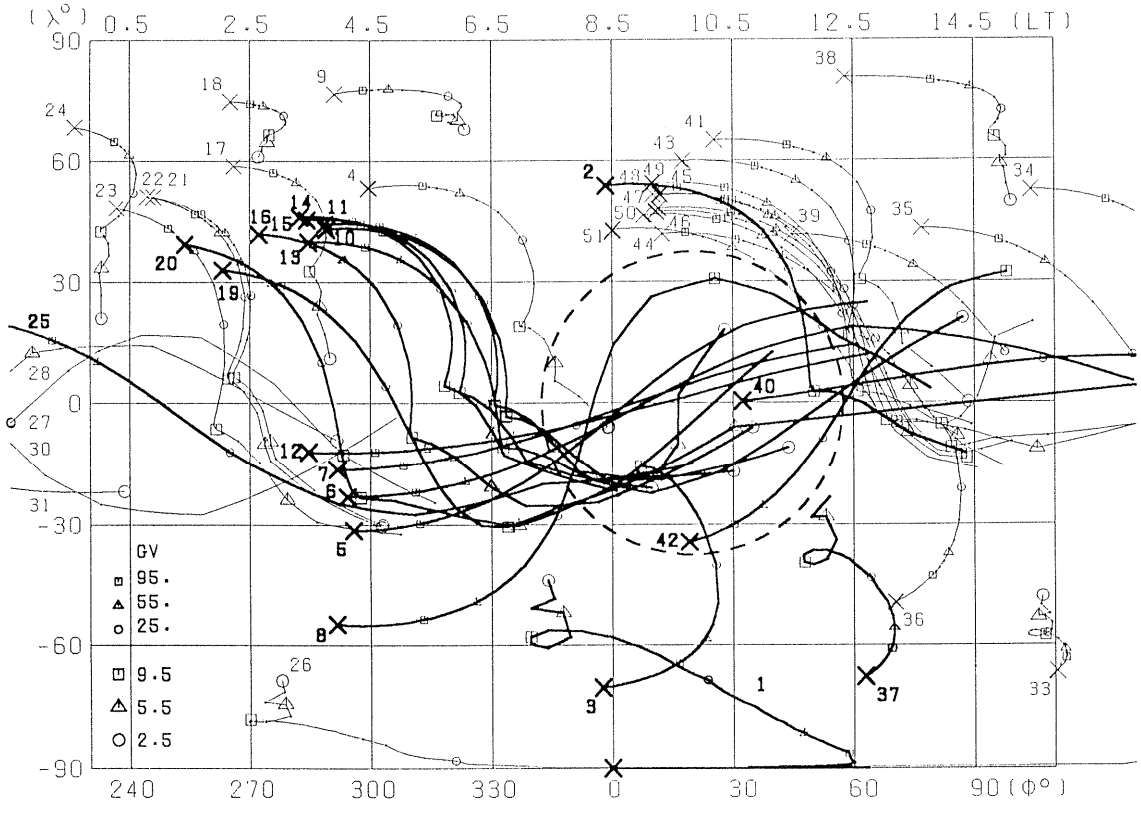

1	SOU:	0.25	11	MTW:	0.77	21	CAL:	0.	31	YAK:	0.
2	LEE:	0.92	12	HUA:	2.22	22	SUL:	0.	32	TIX:	0.
3	SAN:	2.08	13	SWA:	1.81	23	VIC:	0.	33	WIL:	0.
4	GOO:	0.	14	OTT:	0.75	24	INU:	0.	34	IRU:	0.
5	COR:	1.12	15	DEE:	1.00	25	KUL:	0.49	35	ALM:	0.
6	MIN:	2.07	16	CHI:	1.66	26	MCM:	0.	36	KER:	0.
7	CHA:	2.11	17	CHU:	0.	27	BRI:	0.	37	MAW:	0.47
8	USH:	1.95	18	RES:	0.	28	HOB:	0.	38	HEI:	0.
9	THU:	0.	19	DAL:	1.82	29	TER:	0.	39	TBI:	0.
10	DUR:	1.69	20	CLI:	0.88	30	MTN:	0.	40	KAM:	0.61

41	OUL:	0.	
42	HER:	0.20	
43	UPP:	0.	
44	ROM:	0.	
45	HAL:	0.	
46	MUN:	0.	
47	ZUG:	0.	
48	LIN:	0.	
49	KIE:	0.	
50	JUN:	0.	
51	PIC:	0.	

Figure 4. The inference of the direction of the collimated flow from the distribution of the cosmic ray trajectories classified by the thick or thin lines corresponding to the presence or absence of $\Delta I(t)$ at 0830 UT on January 26, 1968. The number attached to the trajectory represents the station name in Table 1, its abbreviation being listed at the footnote together with $|\Delta I_i^{OB}(t = 0830\ \text{UT})|$ in percent. The focusing of almost all the thick lines into the circular region and the detouring of the thin lines around it except for the one at the number 4 station Goose Bay indicate that the collimated flow is confined in this region. As for the determination of the circle ($\lambda_F = 0°$, $\phi_F = 20°$E; radius = 37.5°), see Text. The trajectories are quoted from *Inoue et al.* [1983].

extent of the region and the large modulus ($d\phi/dp$) of the longitudinal spread of those trajectories in these rigidity regions. It is emphasized here that such an elimination of the trajectory has not been made for the quantitative analysis that follows.

The exact determination of the physical properties of the collimated flow, such as the geographic direction (λ_F, ϕ_F), the collimation index (χ_O) and the rigidity spectrum $\{S(p, t)dp\}$ of the constituent cosmic rays, can be made by minimizing the following quantity (Δ^2) by the nonlinear least squares method called SALS [cf. *Nakagawa and Oyanagi*, 1980].

$$\Delta^2 = \sum_{i=1}^{51} w_i\{\Delta I_i^{OB}(t) - \Delta I_i^{EX}(\lambda_F, \phi_F, \chi_O, A, \gamma; t)\}^2 = \text{Min.}, \quad (3)$$

where w_i is the weight derived from the hourly dispersion (σ_h) of the intensity shown in Table 1, $\Delta I_i^{OB}(t)$ is the observed PD inclusive of zero value at the ith station and ΔI_i^{EX} is the corresponding one expected from the collimated flow with the following distribution function $U(\chi, p, t)$:

$$U(\chi, p, t)dp = F(\chi, t) \cdot S(p, t)dp, \quad (4)$$

$$S(p, t)dp = A(t)(p/p_0)^{\gamma(t)}dp/p_0; \qquad p_0 = 1\ \text{GV}, \quad (5)$$

$$F(\chi, t) = 1, \qquad \chi \leq \chi_O(t), \quad (6a)$$

$$F(\chi, t) = 0, \qquad \chi > \chi_O(t), \quad (6b)$$

in which χ is measured from the flow axis ($-\lambda_F$, $-\phi_F$). We calculate ΔI_i^{EX}, taking into account the contribution to the

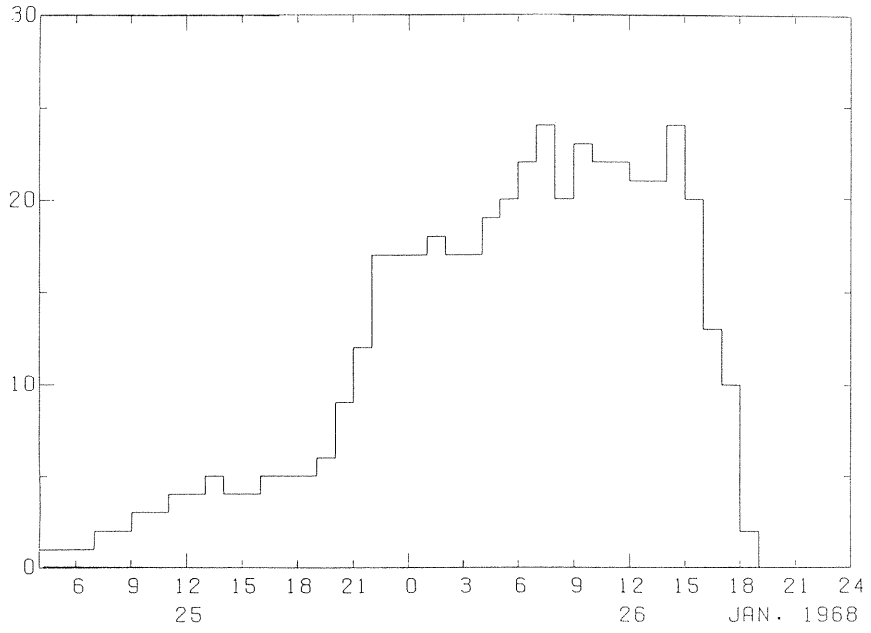

Figure 5. Time distribution of numbers of the stations with a finite $\Delta I_i^{OB}(t)$.

neutron intensity, of the galactic cosmic rays from 9 directions (the vertical and the four cardinal points with the zenith angles of 16° and 32°), their contribution ratio from three zenithal directions (Z = 0°, 16°, and 32°) being assumed to be 1:5.2:3.2 [cf. *McCracken et al.*, 1965]. The total contribution from the nine directions is given by the response function. In the present analysis we use the one obtained by *Nagashima et al.* [1989], which is expressed in the analytical form in terms of the cosmic ray rigidity, the atmospheric depth, and the solar activity. The asymptotic orbits of cosmic rays used here are those obtained by *Inoue et al.* [1983] in the International Geomagnetic Reference Field in 1975 [*Peddie*, 1982]. It is noted that the asymptotic orbits are influenced by the secular variation of the geomagnetic field [cf. *Shea and Smart*, 1990, and references therein], but, as the influence in the high-rigidity region is small, we can use those orbits in 1975 for the present calculation.

The accuracy of the solution strongly depends on numbers of the stations with a finite ΔI_i^{OB} and also on the uniformity of their geographic distribution. Their time distribution is shown in Figure 5. We have analyzed those data in the period from 2200 UT on January 25 to 1600 UT on January 26 and obtained somewhat satisfactory results only in the period of 0300–1100 UT on January 26 as shown in Figure 6. Those results before and after the period are not presented for the following reason, in spite of their unlarge errors. Before the period, the distribution of the flow-observable stations is concentrated only in the northwestern part of the circular region supposed to be covered by the collimated flow. This causes the erroneous or biased solution in spite of a considerable number of the available stations with a nonzero $\Delta I_i^{OB}(t)$. After the period, on the other hand, the stations in the western part of the circular region are scarce, and furthermore some of them observe the FD-affected PD, as pointed out previously. This also causes the erroneous solution. For the demonstration of the appropriateness of the analysis, Figure 7 shows an example of the comparison between ΔI_i^{EX} and ΔI_i^{OB} at 0330 UT on January 26. One can see a fairly good agreement between them.

4. Result and Discussions

The obtained flow bears the following characteristics:

1. The collimated flow is from the direction expressed by the latitude (Λ_F) and longitude (Φ_F) in the Geocentric-Solar-Ecliptic (GSE) coordinates as shown by the solid points in Figure 6. Almost all the directions are in the northern hemisphere. It is added to note that if we express these directions in the geographic coordinates (λ, ϕ), they are all in the southern hemisphere, as has been inferred from the qualitative analysis using the cosmic-ray trajectories on the geographic map in Figure 4. Corresponding to these directions, those expected from the IMF are shown by the rectangular area, its upper and lower limits being, respectively, $\pm 1\sigma$ from the expected value, quoted from *Couzens and King* [1986]. It would be possible to say that the observed directions show rather good agreement with the expected, as the five points in longitude and the seven points in latitude out of each eight are within or near the range of the rectangular area. However, the observed directions show the systematic deviation from the expected; the points in longitude are always greater than the expected and those in latitude are less than the expectation. Such a deviation would be due to the error caused by the incomplete distribution of the worldwide network stations for the analysis or to the difference of the flow-guiding IMF from the observed one at a point, as the cosmic rays would be influenced by the IMF widely distributed in space. Further analysis of other events would be required for the definite conclusion in regard to this matter.

2. Some of the collimation indices (χ_O) obtained by the present analysis are a little greater than those expected from the IMF (cf. equation (1)). This would be due to the following reasons: (1) The expected index is widened by the

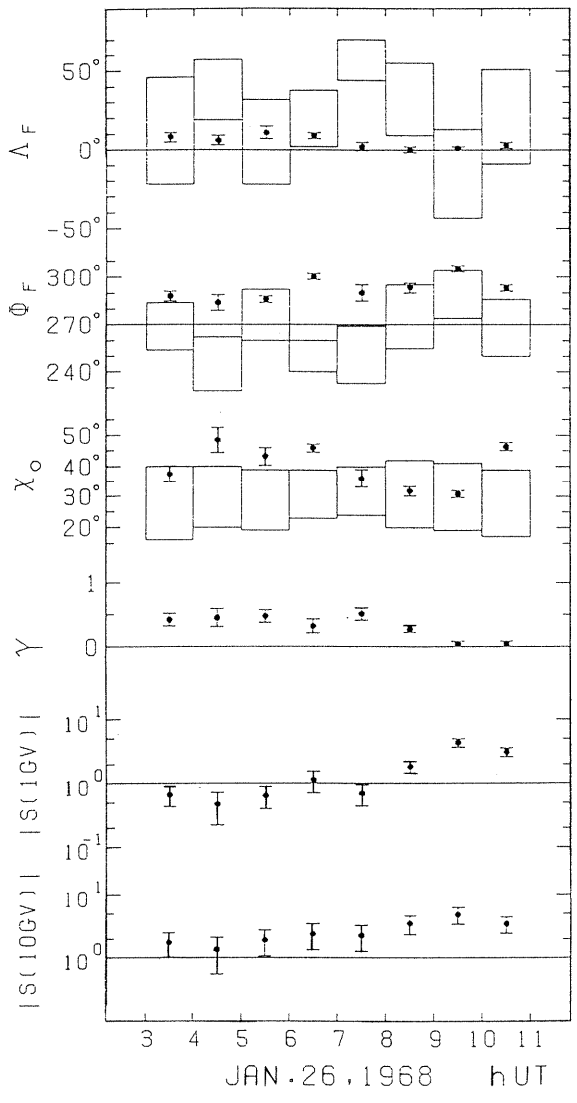

Figure 6. Physical properties of the collimated flow inferred from the precursory decrease on January 26, 1968. $|S(p = 1\ \text{GV}, t)|$ and $|S(p = 10\ \text{GV}, t)|$ are the absolute magnitude of the flow in percent, and γ is the power exponent of the rigidity spectrum (cf. Equation (5)). The latitude (Λ_F) and longitude (Φ_F) of the direction of the flow in the GSE-coordinates and its collimation index (χ_O) obtained by the analysis are plotted by the points, and those expected from the IMF are expressed by the rectangular area, its upper and lower limits being, respectively, $\pm 1\sigma$ from the average value, quoted from *Couzens and King* [1986].

scattering of the cosmic rays with the magnetic irregularities on the way to the Earth from the shock front. (2) The expected index is for $B_S = 15.4$ nT, which is the maximum hourly value at the shock [cf. *Couzens and King*, 1986]. If we could use a little smaller B_S, such as the average magnetic field at the shock, the expected value is increased. (3) B_S and B_O in (1) must be on the same magnetic line of force. In the present calculation this condition is not satisfied. If we could use the correct value of B_S, the expected index might be increased. On the basis of the above consideration it could be concluded that the observed index shows rather good agreement with the expectation. It is added to note that we made a comparative analysis by replacing the anisotropic distribution in (6) with the following one:

$$F(\chi) = \{\cos(\chi/2)\}^n, \qquad n \gg 1, \qquad \pi \geq \chi \geq 0, \quad (7)$$

which is a smoothly varying function of χ, even if the unknown parameter n is very large. It was found that there is nothing to choose between the two from the statistical point of view, and furthermore, the two distributions derive almost the same values of Λ_F, Φ_F and $S(p, t)$. This certifies the orthogonality between the parameters of the spatial distribution and those of the rigidity spectrum in the present analysis. In the present paper we have selected the convex-type anisotropy in (6) for no other reason than that the cosine-type anisotropy in (7) has some ambiguity in defining the collimation index to be compared with the expected value.

3. The power exponent (γ) of the rigidity spectrum is almost zero just prior to the shock front and gradually increases with the increase of the distance of the Earth from the shock. The initial zero value of γ near the front is greater than that ($\gamma \sim -0.5$) of the Fd. This implies that the cosmic rays with higher rigidities more easily pass across the magnetic shock to form the collimated flow, and the passage ability is proportional to $p^{0.5}$. The following increase of γ from 0 to ~0.5 could be regarded as being due to the rigidity dependence of the cosmic ray scattering with the magnetic irregularities outside the shock front.

4. The absolute magnitudes $|S(p, t)|$s of the collimated flow at $p = 1$ GV and 10 GV are shown in Figure 6. $|S(p, t)|$ decreases with the increase of the distance of the Earth from the shock front. This can be regarded as being due to the attenuation effect caused by the magnetic scatterings of the cosmic rays on the way to the Earth from the shock front. As all the points in the figure are approximately on a straight line, the attenuation can be expressed by the exponential function as

$$S(p, t) \propto \exp(\Delta t/\tau_0), \qquad \Delta t \leq 0, \quad (8)$$

where Δt is measured inversely from the commencement of the shock. The decay constant τ_0 in (8) is 3.4 ± 0.7 hours at

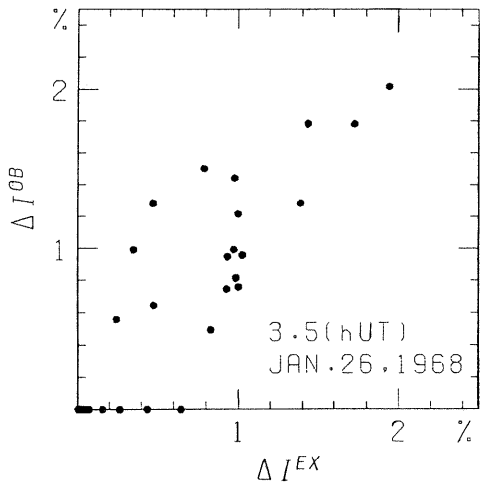

Figure 7. Comparison between the observed and expected precursory decreases at each station at 0330 UT on January 26, 1968.

p = 1 GV and 6.5 ± 1.3 hours at p = 10 GV. The difference between the attenuations at different p values could be interpreted as being due to the rigidity dependence of the magnetic scatterings of the cosmic rays on the way to the Earth from the shock front. It is added to note that these attenuations are considerably smaller than τ_0 = 23.8 hours obtained by the previous analysis of the averaged precursory decrease during 1970–1985 [*Nagashima et al.*, 1992].

5. Conclusion

By analyzing the hourly data of the local-time-dependent precursory decrease from the worldwide network stations on January 25 and 26, 1968, the physical properties of the collimated flow in front of the magnetic shock, produced by the collimation action of the bottle-neck structure of the IMF, have been obtained, as shown in Figure 6. It is noteworthy that the direction and the collimation index of the flow approximately coincide respectively with those expected from the IMF. This fact gives evidence for the reconfirmation of the existence of the IMF-guided collimated flow of the low-density cosmic rays across the shock from the inside of the FD, responsible for the precursory decrease.

Acknowledgments. The authors express their sincere appreciation to the staffs of the World Data Center C2 for Cosmic Rays for providing them the neutron monitor data and also to the members of Cosmic-Ray Section, Solar-Terrestrial Environment Laboratory, Nagoya University for the kind discussion. One of the authors (I.M.) is indebted also to the staffs of Department of Information Management, Asahi University for their kind encouragement and support given to him. All the computations in this work were made at the Computer Center, Nagoya University.

The Editor thanks S. Mori and D. Smart for their assistance in evaluating this paper.

References

Couzens, D. A., and J. H. King, *Interplanetary Medium Data Book*, suppl. bf. 3A, 1977–1985, NSSDC/WDC-A 84-04, National Space Science Data Center, Greenbelt, Md., 1986.

Inoue, A., M. Wada, and I. Kondo, *Cosmic Ray Table, 1, Asymptotic Directions in 1975*, WDC-C2 for Cosmic Rays, Institute of Physics and Chemistry, Itabashi, Tokyo, Japan, 1983.

McCracken, K. G., U. R. Rao, B. C. Fowler, M. A. Shea, and D. F. Smart, Cosmic Ray Tables: Asymptotic directions, variational coefficients and cut-off rigidities, in *IQSY Instruction Manual*, no. 10, IQSY Committee, London, May 1965.

Nagashima, K., S. Sakakibara, K. Murakami, and I. Morishita, Response and yield functions of neutron monitor, galactic cosmic-ray spectrum and its solar modulation, derived from all available world-wide surveys, *Nuovo Cimento Soc. Ital. Fis. C, 12*, 173, 1989.

Nagashima, K., K. Fujimoto, S. Sakakibara, I. Morishita, and R. Tatsuoka, Local-time-dependent pre-IMF-shock decrease and post-shock increase of cosmic rays, produced respectively by their IMF-collimated outward and inward flows across the shock responsible for Forbush decrease, *Planet. Space Sci., 40*, 1109, 1992.

Nagashima, K., S. Sakakibara, and K. Fujimoto, Local-time-dependent pre-IMF-shock decrease of cosmic rays, produced by their IMF-collimated outward flow across the shock from the inside of Forbush decrease, *J. Geomagn. Geoelectr., 45*, 535, 1993.

Nakagawa, T., and Y. Oyanagi, Program system SALS for nonlinear least-squares fitting in experimental sciences, in *Recent Developments in Statistical Inference and Data Analysis*, p. 221, North-Holland, New York, 1980.

Peddie, N. W., International geomagnetic reference field: The third generation, *J. Geomagn. Geoelectr., 34*, 309, 1982.

Shea, M. A., and D. F. Smart, The influence of the changing geomagnetic field on cosmic ray measurements, *J. Geomagn. Geoelectr., 42*, 1107, 1990.

K. Fujimoto and K. Nagashima, Cosmic-Ray Section, Solar-Terrestrial Environment Laboratory, Nagoya University, Nagoya 461-01, Japan. (e-mail: fujimoto@stelab.nagoya_u.ac.jp)

I. Morishita, Department of Information Management, Asahi University, Hozumi-cho, Motosu-gun, Gifu 501-02, Japan. (e-mail: isao@alice.ashi_u.ac.jp)

(Received June 7, 1993; revised February 14, 1994;
accepted April 5, 1994.)